

## Cover Page

**Title:** Glutamate-Induced Electrical and Calcium Signals in the Moss *Physcomitrella patens*

**Short title:** Glutamate-induced signals in *Physcomitrella*

**Corresponding author:** M. Koselski

Department of Plant Physiology and Biophysics, Institute of Biological Sciences, Maria Curie-Skłodowska University, Akademicka 19, Lublin/20-033, Poland, Telephone: (+48)815375955, Email address: mateusz.koselski@poczta.umcs.lublin.pl

**Subject areas:** cell–cell interaction, membrane and transport

**Number of black and white figures:** 0

**Number of colour figures:** 8

**Number of tables:** 1

**Number of supplementary material:** 8 videos

## Title Page

**Title:** Glutamate-Induced Electrical and Calcium Signals in the Moss *Physcomitrella patens*

**Short title:** Glutamate-induced signals in *Physcomitrella*

Mateusz Koselski\*, Piotr Wasko<sup>1</sup>, Kamil Derylo<sup>2</sup>, Marek Tchorzewski<sup>2</sup>, Kazimierz Trebacz<sup>1</sup>

<sup>1</sup>Department of Plant Physiology and Biophysics, Institute of Biological Sciences, Maria Curie-Skłodowska University, Lublin, 20-033 Poland

<sup>2</sup>Department of Molecular Biology, Institute of Biological Sciences, Maria Curie-Skłodowska University, Lublin, 20-033 Poland

**Corresponding author:** Mateusz Koselski

Email address: [mateusz.koselski@poczta.umcs.lublin.pl](mailto:mateusz.koselski@poczta.umcs.lublin.pl)

## Abstract

The mode of transmission of signals between plant cells is an important aspect of plant physiology. The main role in generation of long-distance signals is played by changes in the membrane potential and cytoplasmic calcium concentration, but the relation between these responses evoked by the same stimuli in the same plant remains unknown. As one of the first plant which colonized lands, the moss *Physcomitrella patens* is a suitable model organism for studying the evolution of signaling pathways in plants. Here, by application of glutamate as a stimulus, we demonstrated that electrical but not calcium signals can be true carriers of information in long-distance signaling in *Physcomitrella*. Generation of electrical signals in a form of propagating transient depolarization seems to be dependent on the opening of calcium channels, since the responses were reduced or totally blocked by calcium channel inhibitors. While the microelectrode measurements demonstrated transmission of electric signals between leaf cells and juvenile cells (protonema), the fluorescence imaging of cytoplasmic calcium changes indicated that calcium response occurs only locally - at the site of glutamate application, and only in protonema cells. This study indicates different involvement of glutamate-induced electrical and calcium signals in cell-to-cell communication in these evolutionarily old terrestrial plants.

**Keywords:** calcium imaging, glutamate, long-distance signaling, membrane potential, *Physcomitrella patens*

## Introduction

One of the most important periods in the history of the biosphere was the colonization of terrestrial habitats by plants. Bryophytes, i.e. the first plants that appeared on the land, evolved from aquatic ancestors resembling charophytes - freshwater algae. During the conquest of land, plants required adaptation of their signaling systems to land-specific environmental stress factors like UV radiation, sudden temperature changes, drought, wounding, etc. The moss *Physcomitrella patens* was chosen as one of the models of early terrestrial plants. Its simple structure and fully sequenced genome as well as the relative ease of obtaining different mutants by homologous recombination facilitated this choice (Cove, 2000; Rensing et al., 2008). For approximately three decades, *P. patens* has attracted attention of researchers interested in plant signaling. Two aspects of long-distance signaling processes: calcium waves and action potential-like responses have been addressed in numerous publications. Ermolayeva and co-workers (Ermolayeva et al., 1997, 1996; Johannes et al., 1997) registered transient depolarization resembling action potentials (APs) in response to red light pulses in protonema cells of *P. patens*. After approximately 3 days, these signals induced morphogenetic changes - formation of side branch initials or, less frequently, formation of buds, which developed into gametophores. The AP-like responses involved a calcium component and were reduced by calcium channel inhibitors (Ermolayeva et al., 1997) or blocked after removal of external calcium (Ermolayeva et al., 1996; Johannes et al., 1997). An increase in the cytoplasmic calcium concentration  $[Ca^{2+}]_{cyt}$  in protonema cells was also demonstrated in experiments carried out on plants transformed with apoaquorin cDNA, where the effect of blue light, mechanical perturbation, cold shock, application of a solution with low pH (3.5), and heat shock were studied (Russell et al., 1998, 1996; Saidi et al., 2009). An increase in  $[Ca^{2+}]_{cyt}$  in a form of calcium waves was also recorded after UV-A using fura-2dextran (Tucker et al., 2005).

In contrast to protonema cells, which are an early stage of moss development, the electric signals in the leaves of a gametophyte are more complex (Koselski et al., 2008). Illumination evoked APs of all-or-none character. Unexpectedly, AP-like transient depolarizations were also registered upon darkening. They lasted extremely long – approx. 20 minutes. Application of  $La^{3+}$  (5 mM) blocked both these types of responses, which again pointed to involvement of  $Ca^{2+}$  fluxes in generation of these signals (Koselski et al., 2008).

Gametophytes of *P. patens* also respond to local cold stress with transient depolarization of the membrane potential, which is transmitted with decrement to neighboring cells (Koselski et al., 2019). This response is not sensitive to externally applied gadolinium (5 mM) but is enhanced upon treatment with  $\text{Sr}^{2+}$ , which is assumed to liberate  $\text{Ca}^{2+}$  from internal stores (Koselski et al., 2019).

$\text{Ca}^{2+}$ -transients appearing in response to different stress factors were visualized in *P. patens* with the use of different optical techniques (Haley et al., 1995; Russell et al., 1996; Saidi et al., 2009; Tucker et al., 2005). Recently, calcium imaging in *P. patens* has reached a new level, owing to the successful transformation with FRET-based Cameleon YC3.60 (Storti et al., 2018) and GCaMP3 (Kleist et al., 2017). Both these studies address the response to osmotic stress - an important adaptation mechanism during land colonization (Kleist et al., 2017; Storti et al., 2018). It was demonstrated that osmotically-induced  $\text{Ca}^{2+}$  waves propagated throughout entire young gametophores of *P. patens* with a speed of approx.  $4 \mu\text{ms}^{-1}$  (Storti et al., 2018). The amplitudes of the waves were only slightly reduced upon substitution of external  $\text{Ca}^{2+}$  with  $\text{La}^{3+}$ , indicating possible involvement of intracellular  $\text{Ca}^{2+}$  stores in these signals (Storti et al., 2018).

In the present study, we combine electrophysiological techniques and  $\text{Ca}^{2+}$  imaging to study the responses of *P. patens* to glutamate (Glu) treatment. The occurrence of Glu in a plant environment is regarded as a signal of wounding or as an indication of a source of nutrients. We demonstrate in GCaMP3-transformed protonema of *P. patens* (Kleist et al., 2017) that Glu-induced  $\text{Ca}^{2+}$  transients appear only locally and do not propagate, in contrast to electrical signals, which are transmitted throughout the plant.

## Results

### Electrical signals in leaf cells

The microelectrode measurements showed that application of 5 mM glutamate to the basal part of the moss (from the rhizoid side) evoked transient depolarization of the membrane potential which propagated to leaf cells located in the apical part of the moss (Fig. 1). Depolarizations of the membrane potential started during the first second of the stimulation and were recorded even 4 mm from the site of stimulation (the distance between the barrier that separated the stimulated part of the plant and the microelectrode insertion site was between 1.3 and 4 mm). Starting from

the initial value of the membrane potential ( $V_0$ ), which amounted to  $-163 \pm 3$  mV ( $n=26$ ), the depolarization of the membrane proceeded at the rate ( $R_{\text{dep}}$ ) of  $13.5 \pm 2.3$  mV/s ( $n=26$ ) and reached the maximum value of the membrane potential ( $V_{\text{max}}$ ) at  $-104 \pm 4$  mV ( $n=26$ ). The amplitude of the depolarization ( $A$ ) amounted to  $59 \pm 4$  mV ( $n=26$ ) and the duration of the response measured at half of the amplitude ( $t_{1/2}$ ) was  $154 \pm 12$  s,  $n=26$ . Besides the responses propagating from the basal part of the moss to the apical part (acropetal), an opposite direction of propagation (basipetal) was observed as well (Fig. 1, Table 1). In contrast to the acropetally propagating responses, basipetal propagation was not recorded in every tested plant; hence, only responses starting from the basal part of the moss were studied in relation to calcium ion fluxes.

The membrane potential changes evoked by glutamate were dependent on the glutamate concentration (Fig. 2, Table 1). The responses evoked by different glutamate concentrations (0.05 mM, 0.5 mM, and 30 mM) were compared to that obtained at 5 mM glutamate. At 0.05 mM and 0.5 mM glutamate, a negative shift of  $V_{\text{max}}$  was observed; the values of the membrane potential reached  $-127 \pm 8$  mV ( $n=6$ ) and  $-130 \pm 9$  mV ( $n=8$ ), respectively. Not every plant generated responses after 0.05 mM and 0.5 mM glutamate; 0.05 mM glutamate was effective in 60% (the response was recorded in 6 of the 10 tested plants), whereas the effectiveness of the 0.5 mM glutamate application reached 80% (8 out of the 10 tested plants responded). Moreover, the amplitude of the responses after the 0.5 mM glutamate treatment was significantly lower than at the other concentrations ( $A$  reached  $38 \pm 7$  mV;  $n=8$ ). Statistically significant differences were also recorded in  $R_{\text{dep}}$ , which increased together with the glutamate concentration; at 0.05 mM, 0.5 mM, and 30 mM,  $R_{\text{dep}}$  amounted to  $0.22 \pm 0.04$  mV/s ( $n=6$ ),  $1 \pm 0.3$  mV/s ( $n=8$ ), and  $23.1 \pm 3.6$  mV/s ( $n=13$ ), respectively. The last statistical significant difference was found in  $t_{1/2}$  of the responses evoked by 30 mM, which lasted longer ( $t_{1/2}$  amounted to  $290 \pm 33$  s,  $n=14$ ) than after the application of the lower glutamate concentrations (Table 1). Taking into account the effectiveness and saturation of the amplitude of responses recorded after the application of 5 mM glutamate, we applied this concentration of glutamate in the other analyses in our study.

To study the involvement of the glutamate receptor in glutamate-evoked responses, DNQX, i.e. an antagonist of ionotropic AMPA and kainate receptors, was applied. After conditioning of the basal part of the moss in 0.2 mM DNQX, the application of glutamate in this part of the plant still

evoked responses in the leaf cells from the apical part of the plant. The DNQX treatment caused reduction of  $A$  and shift of  $V_0$  to more positive values (Fig. 1, Table 1).

The specificity of the glutamate-induced responses was tested by application of a structurally similar compound - aspartate. In contrast to glutamate, aspartate was not effective in evoking membrane potential changes. Neither long-distance nor local membrane potential changes were recorded after the aspartate treatment, regardless of the place of aspartate application - the basal part of the plant located opposite to the microelectrode insertion or close to the microelectrode (Fig. 3).

Calcium dependence of the responses was studied by immersion of the basal part of the plant in the standard solution supplemented with different calcium channel inhibitors (5 mM gadolinium, 100  $\mu$ M verapamil, 40  $\mu$ M tetrandrine, 100  $\mu$ M nifedipine), a calcium chelator (0.4 mM EGTA), or by 20-fold reduction of extracellular calcium (Fig. 1, Table 1). The most effective of the calcium channel inhibitors used was verapamil, which totally inhibited the responses. The only effect of verapamil was a shift of  $V_0$  to more negative values ( $-180 \pm 3$  mV  $n=14$ ). Gadolinium was less effective in the blockage of the responses, since they were recorded in 10 of the 14 tested plants. The same inhibitor also evoked many other effects, including reduction of  $A$  to  $34 \pm 4$  mV ( $n=10$ ), a shift of  $V_0$  to more positive values ( $144 \pm 5$  mV,  $n=10$ ), 20-fold reduction of  $R_{\text{dep}}$  (to  $0.5 \pm 0.1$  mV/s,  $n=10$ ), and an increase in  $t_{1/2}$  to  $246 \pm 53$  s ( $n=7$ ). Reduction of  $A$ ,  $R_{\text{dep}}$ , and  $t_{1/2}$  was recorded after addition of tetrandrine: the values of these parameters were  $41 \pm 6$  mV ( $n=12$ ),  $1.4 \pm 0.3$  ( $n=12$ ), and  $97 \pm 9$  ( $n=11$ ), respectively. Nifedipine did not change the parameters significantly.

The significance of extracellular calcium in the response to glutamate was confirmed by the effects of the EGTA application. A decrease in  $A$  to  $33 \pm 6$  mV, ( $n=9$ ), a positive shift of  $V_0$  to  $-134 \pm 7$  mV ( $n=9$ ), reduction of  $R_{\text{dep}}$  to  $1.1 \pm 0.4$  mV/s ( $n=9$ ), and an increase in  $t_{1/2}$  to  $457 \pm 82$  s ( $n=7$ ) were observed. Moreover, in the presence of EGTA, the responses were recorded only in 9 of the 16 tested plants. Interestingly, after the 20-fold reduction of extracellular calcium in the standard solution (to 50  $\mu$ M) applied on both sides of the plant, the responses were evoked in every tested plant. Besides, at the 50  $\mu$ M concentration of extracellular calcium, glutamate stimulation evoked depolarization of the membrane potential to more positive values ( $V_{\text{max}}$

amounted  $-75 \pm 6$  mV,  $n=12$ ) than in the standard conditions, and the amplitude and duration of the responses increased (A amounted  $85 \pm 5$  mV,  $n=12$  and  $t_{1/2} - 334 \pm 47$  s,  $n=11$ ).

Since the membrane potential changes in plant cells are dependent mainly on potassium and anion fluxes, we intended to determine whether an increase in external  $K^+$  and  $Cl^-$  could affect the glutamate-evoked responses (Fig. 4, Table 1). The increase in the  $Cl^-$  concentration in the batch by addition of 15 mM choline chloride did not evoke any statistically significant differences between the responses. In turn, the addition of 10 mM potassium gluconate evoked a decrease in  $V_0$  (to  $-150 \pm 3$  mV,  $n=10$ ), a positive shift of  $V_{max}$  (to  $-45 \pm 4$  mV,  $n=10$ ), and an increase in A (to  $105 \pm 5$  mV,  $n=10$ ) and  $t_{1/2}$  (to  $393 \pm 39$  s,  $n=8$ ). In 3 of the 13 tested plants, the high external  $K^+$  concentration caused a permanent depolarization of the cell membrane to  $-59 \pm 14$  mV ( $n=3$ ), which could be interrupted by glutamate stimulation (see the right side of the lower panel in Fig. 4). Such responses were not included in the statistical analysis.

### **Electrical signals in protonema cells**

The microelectrode measurements carried out on protonema cells indicated that glutamate evoked depolarization of the cells, which propagated to neighboring cells (Fig. 5). The study of the propagation of the responses consisted in application of glutamate to a thread-like chain of protonema cells at some distance from the cell in which the microelectrode was inserted. The solution in the micropipette used for stimulation with glutamate was stained with 1 mM methyl blue, which allowed observing the spread of glutamate and the moment of its contact with the protonema cells. Immediately after the contact of the first few cells from the chain with glutamate, fast depolarization of the membrane potential ( $23.3 \pm 4$  mV/s,  $n=9$ ) was recorded in a cell located away from the stimulation site (Supplementary Video S1). Such propagating responses had lower amplitude ( $44 \pm 3$  mV,  $n=9$ ) than the responses recorded in the leaf cells. In 4 of the 9 tested plants, fast repolarization of the membrane potential was observed, and the responses were short lasted spikes shown in Fig. 5 ( $t_{1/2}$  of the responses was  $4.8 \pm 1.3$  s,  $n=4$ ). As the micropipette injecting glutamate was shifted to other cells located closer the microelectrode, the next depolarization was observed. The further approach of the injection micropipette to the microelectrode and the direct contact of glutamate with the cell in which the microelectrode was inserted resulted in an increase in the amplitude of the response and a plateau of the membrane potential.

## Calcium signals

The influence of glutamate on  $\text{Ca}^{2+}$  changes in cells was determined in transgenic plants expressing GCaMP3, which were previously used to study  $[\text{Ca}^{2+}]_{\text{cyt}}$  changes after salinity and touch by Kleist and coworkers (Kleist et al., 2017). The stimulation consisted of placement of a drop of a standard solution supplemented with glutamate on leaves or protonema. The stimulation resulted in an increase in the fluorescence observed in the protonema cells (Fig. 6, Supplementary Video S3), but not in the leaf cells (Supplementary Video S4). Similar to the electrical signals, the calcium signals were specific responses to glutamate but not to aspartate (Supplementary Video S5). Contact of the protonema cells located on the surface of an agar plate with glutamate resulted in an instant increase in the fluorescence intensity in the cells. In the first seconds after the application of glutamate, an increase in the fluorescence intensity was recorded only in the region covered by the drop. After several dozen seconds, a certain spread of the drop was observed and a slow increase in fluorescence in cells located under the drop. Such results suggested the absence of propagation of calcium signals in the protonema cells. To study the possibility of calcium propagation in protonema cells in more detail, we decided to make measurements of single protonema cells using an injection micropipette for application of glutamate (Fig. 7, Supplementary Video S6). Such focused application of glutamate indicated that calcium signals were not propagated from cell to cell, because an increase in fluorescence was recorded only in cells in contact with glutamate.

The ability of glutamate-induced calcium signals to propagate was also studied using the non-invasive MIFE method. The measurements were carried out on 12 plants and proved that the application of glutamate to the basal part of the plant did not evoke changes in the net  $\text{Ca}^{2+}$  flux in apical leaf cells (Fig. 8).

## Discussion

In the present study, we considered electrical and calcium signals after application of glutamate, i.e. an amino acid playing a role of a neurotransmitter in the animal nervous system. In *Physcomitrella*, the involvement of glutamate receptors in cell-to-cell signaling is still unknown, whereas the involvement of the receptors in chemotaxis and reproduction in the moss has been well documented to date (Ortiz-Ramirez et al., 2017).

The first plant genes coding for ionotropic glutamate receptors (iGluRs) were found in *Arabidopsis thaliana* (Lacombe et al., 2001; Lam et al., 1998). While glutamate receptors in *Arabidopsis* are encoded by 20 genes, only two GLR genes have been found in the *Physcomitrella* genome (Verret et al., 2010). Phylogenetic analysis performed by De Bortoli and coworkers (De Bortoli et al., 2016) showed that the genes of glutamate receptors in *Physcomitrella* are in the same clade as AtGLR3.4 and AtGLR3.5. Experiments carried out on *Arabidopsis* glutamate receptors of family 3 confirmed the effectiveness of the DNQX antagonist of animal glutamate receptors (Li et al., 2013; Meyerhoff et al., 2005; Teardo et al., 2010). It was also shown that one of the receptors of family 3, AtGLR3.3, plays the main role in glutamate-evoked depolarizations (Qi et al., 2006). In our study, DNQX reduced but not totally blocked the amplitude of glutamate-evoked membrane potential changes, rising questions of DNQX specificity in the case of glutamate receptors in *P. patens*. On the other hand, the specificity of glutamate as a stimulus seems to be high, since neither electrical nor calcium signals were recorded after application of a structurally close compound, i.e. aspartate (Fig. 3., Supplementary Video S5).

Glutamate-evoked changes in the membrane potential were previously recorded in different plants including *Arabidopsis thaliana* (Dennison and Spalding, 2000; Meyerhoff et al., 2005; Qi et al., 2006; Sivaguru et al., 2003), *Hordeum vulgare* (Felle and Zimmermann, 2007), and plants studied in our laboratory - *Helianthus annuus* (Stolarz et al., 2015, 2010) and the liverwort *Conocephalum conicum* (Król et al., 2007). Apart from *Arabidopsis*, the membrane potential changes evoked by glutamate in every plant mentioned above were in a form of APs. Moreover, it was demonstrated that APs in *Hordeum* and *Helianthus* were able to propagate. The involvement of  $\text{Ca}^{2+}$  in glutamate-evoked membrane potential changes was well documented in *Arabidopsis*, *Hordeum*, and *Conocephalum* to proceed mainly by blockage of the responses by inhibitors of calcium-permeable channels. In analyses of aequorin-expressing seedlings, Dennison and Spalding, (2000) demonstrated that the glutamate-induced influx of  $\text{Ca}^{2+}$  into the cell occurs before membrane potential changes and lasts only up to a dozen of seconds. Similarly, calcium influx to the cell seems to be crucial in generation of the glutamate-induced responses recorded in our study, since the membrane potential changes were reduced or completely blocked in the presence of calcium channel inhibitors or the  $\text{Ca}^{2+}$  chelator - EGTA (Fig. 1, Table 1). On the other hand, the results obtained at the low calcium concentration in the medium (50  $\mu\text{M}$ ) were

surprising, as in such conditions higher amplitudes and duration of the responses were recorded in such conditions than in the control (in the presence of 1 mM extracellular  $\text{Ca}^{2+}$ ). The calcium dependence was not evident in our previous studies carried out on *Physcomitrella* leaf cells, since an increase in the amplitude of light- and dark-induced APs was recorded after removal of extracellular  $\text{Ca}^{2+}$  and the increase in the calcium concentration resulted in loss of excitability (Koselski et al., 2008). Later studies demonstrated that cold- and menthol-induced membrane potential changes in *Physcomitrella* can be recorded in the presence of the  $\text{Gd}^{3+}$  calcium channel inhibitor and in the absence of cytoplasmic calcium (Koselski et al., 2019). Probably, the optimal amplitude of the response requires some optimal calcium concentration, which can be finely tuned by the activity of calcium channels from the plasma membrane and/or internal stores.

Although the initiation of glutamate-induced electrical signals in *Physcomitrella* is dependent on an influx of external  $\text{Ca}^{2+}$ , depolarization of the plasma membrane seems to be dependent on  $\text{K}^+$  fluxes (Fig. 4, Table 1). The efflux of  $\text{Cl}^-$  from the cell during depolarization of the plasma membrane, which is a known phenomenon in many plant species, including the liverwort *Conocephalum conicum* studied in our lab (Trebacz et al., 1994), does not seem to be crucial for glutamate-induced depolarization in *Physcomitrella*. After the 6-fold increase in the external  $\text{Cl}^-$  concentration, we recorded only a slight (4 mV) shift of  $V_{\text{max}}$ , which should reach 45 mV in accordance with the Nernst law if the membrane were permeable only for  $\text{Cl}^-$ . It seems that the most important event for reaching  $V_{\text{max}}$  is the opening of potassium channels, because a shift to positive values of the membrane potential after the 11-fold increase in the external  $\text{K}^+$  concentration reached 59 mV, i.e. an almost the same value as that calculated from the Nernst equation. Probably, potassium channels can be opened for a long time and, consequently, we observe a plateau of the membrane potential, whose level and duration can be dependent on the external  $\text{K}^+$  concentration. Such long-lasting high permeability of the cell membrane for potassium is known from *Chara* as the "K-state" (Beilby, 1985, Beilby, 1986; Tester, 1988). In *Physcomitrella*, a long-lasting plateau is a common phenomenon for membrane potential changes occurring not only after glutamate treatment but also after application of other kinds of stimuli tested in our lab, e.g. menthol (Koselski et al., 2019) and darkening (Koselski et al., 2008). The long-lasting increase in  $\text{K}^+$  permeability can mask the effect of transient opening of  $\text{Cl}^-$  and  $\text{Ca}^{2+}$  permeable channels. One of the effects of the increase in the external  $\text{K}^+$  concentration was also the change in the shape of depolarization, which was not as "sharp" as in standard conditions. A

characteristic trait of the responses was the slower final part of depolarization, which may be a result of opening of potassium channels taking part in the plateau of the membrane potential. Probably, the opening of potassium channels is slower than the opening of other channels responsible for depolarization of the cell membrane. The slow kinetics of activation of potassium channels may be hidden in standard conditions when  $V_{\max}$  is close to the equilibrium potential for potassium and is achieved by opening of other than potassium channels having fast kinetics of activation.

One of the most crucial aims of our study was to investigate the capabilities of electrical and calcium signals to propagate. While the involvement of glutamate receptors in propagation of long-distance electrical and calcium signals in plants is well documented (Mousavi et al., 2013; Salvador-Recatalà et al., 2014; Toyota et al., 2018; Wang et al., 2019), glutamate-induced systemic responses were recorded in our study only in the case of electrical signals (Fig. 1-5, Supplementary Video S1), but calcium signals were recorded locally (Fig. 6, 7, Supplementary Videos S3 and S6). The absence of propagation of calcium signals was confirmed in the experiments carried out on protonema cells consisting in fluorescence measurements (Fig. 6 and 7, Supplementary Video S3 and S6) and recording of  $\text{Ca}^{2+}$  fluxes in MIFE experiments (Fig. 8). The lack of glutamate induced systemic calcium waves in *Physcomitrella* but not in the higher plant *Arabidopsis* could indicate evolution of such response. One of the main determinants of the presence of systemic calcium waves can be the strength or kind of the stimulus. Apparently, glutamate is a weaker stimulus in comparison to such damaging or strong stimuli as wounding and high osmotic shock used by Toyota et al. (2018) and Storti et al. (2018). Besides the strength of the stimulus, another condition for calcium wave propagation can be the age of tested cells. It is probable that the abundance of glutamate activated calcium channels in *Physcomitrella* is changing during the development of the plant - the density of the channels is high in the protonema but decreases in mature leaf cells. In younger cells, the transmission of calcium signals and/or sensitivity to stimuli can be better; hence, the glutamate-evoked changes in  $[\text{Ca}^{2+}]_{\text{cyt}}$  were recorded only in the protonema cells, which are part of the juvenile tissue of the gametophyte. Different sensitivity to osmotic stress of different cell types was earlier demonstrated by Storti et al. (2018), where changes in  $[\text{Ca}^{2+}]_{\text{cyt}}$  were not recorded in adult cells - phyllids. Some evidence for the importance of the cell age and stimulus strength for signal perception and transmission was provided in the experiments carried out in our lab on GCaMP3

mutants. It was shown that strong deflection of the stem (mechanical stimulus) evoked an increase in the fluorescence in the basal part of the plant (Supplementary Video S8), but glutamate application onto leaves did not change the fluorescence (Supplementary Video S4).

In the present study, we have demonstrated that glutamate-induced electric but not calcium signals are long-distance responses. Probably, the age of cell and kind of stimuli are most important for transmission of electrical and calcium signals. While weak or non-damaging stimuli are efficient to evoke electrical signals, the information about strong or damaging stimuli can be carried from cell to cell with the aid of calcium waves.

## Material and methods

### Plant material

The gametophytes of the moss *Physcomitrella patens* were grown in Petri dishes on solid agar medium KNOP (Reski and Abel, 1985). The conditions in the growth chamber (Convion Adaptis A1000, Convion, Winnipeg, Canada) were set as follows: temperature 23 °C, light intensity 60  $\mu\text{mol}/\text{m}^2\cdot\text{s}$ , and 16/8 light/dark photoperiod. Two types of plants were used in the experiments - the wild type and GCaMP3 mutants. The wild type plants were used for microelectrode measurements of the membrane potential in leaf cells and for MIFE measurements. The GCaMP3 mutants were used for microelectrode measurements of the membrane potential in protonema cells and for fluorescent imaging of calcium concentration changes.

### Membrane potential measurements carried out on leaf cells

Microelectrode measurements were performed in a 30-mm diameter plastic Petri dish equipped with a dividing barrier diving the plant into two parts - apical and basal. Before measurements, the moss was placed in a small gap in the barrier (about 1 mm width) and sealed with vaseline, which prevented the solutions from mixing. The tightness of the two separate compartments of the Petri dishes was tested by applying different volumes of the solutions - 3 ml at the site of insertion of the microelectrode (inserted into the leaf cell from the apical part of the plant) and 2 ml at the site of application of glutamic acid (applied on the rhizoid side). Only dishes in which

no changes in the volume of the solutions were observed were used for the experiments. The experiments started after 3-5 hours of conditioning of the moss in the bath solutions containing 1 mM KCl, 1 mM CaCl<sub>2</sub>, 50 mM sorbitol, buffered by 2 mM Hepes/Tris to pH 7.5. During conditioning and measurements, the moss was kept in light with the intensity of 60 μmol/m<sup>2</sup>\*s. 500 μl of the bath medium supplemented with 5 mM glutamic acid buffered to pH 7.5 by Hepes/Tris was used for the stimulation. The influence of the different substances used in this study (ion channel inhibitors, EGTA) on glutamate-evoked responses was tested by application of the substances only in one compartment of the Petri dish, i.e. the glutamate-stimulated rhizoid side. The variant of experiments with a 20-fold reduced Ca<sup>2+</sup> concentration (the same conditions were applied for MIFE measurements) consisted of application of the same solution in both compartments of the Petri dish. Ag/AgCl<sub>2</sub> microelectrodes were equipped with micropipettes made from borosilicate glass capillaries (1B150F-6, WPI, Sarasota, USA) and filled with 100 mM KCl. The capillaries were pulled with a micropipette puller P-30 (Shutter Instrument Co., Novato, USA). The microelectrode was positioned by a micromanipulator Sensapex SMX (Oulu, Finland). The region of insertion of the microelectrode was observed using a stereomicroscope Olympus SZ 1145 (Tokyo, Japan). The Ag/AgCl<sub>2</sub> reference electrode was coated with a tube containing a porous tip and filled with 100 mM KCl. Both electrodes were connected to an electrometer FD 223 (World Precision Instruments, Sarasota, USA). A Lab-Trax-4 device (World Precision Instruments, Sarasota, USA) working under LabScribe3 software (World Precision Instruments, Sarasota, USA) was used for data acquisition. The frequency of the sample collection was 2Hz. The LabScribe3 software allowed measurement of the amplitude of the responses (A), rate of depolarization (R<sub>dep</sub>) determined as an interval between the initial moment of depolarization and the half value of the amplitude, time of the responses measured at half of the amplitude (t<sub>1/2</sub>), initial value of the membrane potential measured before stimulation (V<sub>0</sub>), and maximum value of the membrane potential obtained after stimulation (V<sub>max</sub>). Statistical analysis was performed in SigmaStat 4.0 (Systat Software Inc. California, USA). Glutamate-evoked fluctuations of the membrane potential not exceeding 5 mV were regarded as the absence of response and were not included. Figures showing recordings of changes in the membrane potential were prepared using Sigma Plot 9.0 (Systat Software Inc. California, USA), CorelDraw 12 (Corel Corporation, Ottawa, Canada).

Membrane potential measurements carried out on protonema cells

Before the experiments, the moss was conditioned as in the experiments carried out on leaf cells. The microelectrode was mounted on a micromanipulator PatchStar (Scientifica, East Sussex, United Kingdom) and connected to the electrometer Duo 773 (World Precision Instruments, Sarasota, USA). The sampling rate was 5 samples per second. The insertion of the microelectrode into the cell was observed under a microscope Olympus IX71 (Tokyo, Japan). Glutamate was applied with a micropipette made from borosilicate glass capillaries (TW150-4, World Precision Instruments, Sarasota, USA) pulled by a DMZ puller (Zeitz-Instruments Vertriebs GmbH, Martinsried, Germany). The internal diameter of the tip of the micropipette was approx. 6  $\mu\text{m}$ . The glutamate was applied to the cell surface by a microinjector (CellTram vario, Eppendorf, Hamburg, Germany). To observe the propagation of glutamate, the solution in the micropipette was stained with 1 mM methyl blue. The effects of the addition of 1 mM methyl blue to the standard solution are presented in Supplementary Video S2. They were also tested during fluorescence measurements (Supplementary Video S7). The application of glutamate was observed by a camera connected to the microscope (Artcam-500MI, Tokyo, Japan) working with QuickPhoto Camera software (version 2.3, Promicra, Prague, Czech Republic). Screen recordings of live view from the camera together with the cell membrane potential changes visible in LabScribe3 software were made by OBS software (version 23.2.1, Open Broadcaster Software, Massachusetts, USA).

#### MIFE measurements

The MIFE (microelectrode ion flux estimation) experiments were performed in the chamber used for the microelectrode experiments - a Petri dish divided into two compartments. The standard solution differed from that used in the microelectrode measurements in its calcium concentration - 50  $\mu\text{M}$   $\text{CaCl}_2$  was used instead of 1 mM. As in the microelectrode measurements, the moss was conditioned 3-5 hours before the start of the experiments. The net  $\text{Ca}^{2+}$  fluxes were obtained with the use of calcium-selective microelectrodes. The electrode diameter was approx. 3  $\mu\text{m}$ . The tip of the electrodes was filled with calcium ionophore (calcium ionophore I - cocktail A, Sigma-Aldrich, Missouri, USA) and backfilled with 200 mM  $\text{CaCl}_2$ . The electrodes were calibrated in solutions with known  $\text{Ca}^{2+}$  concentrations before use in the experiments. Only responses of the electrodes higher than 25 mV/pCa were accepted. The reference electrode was the same as in the microelectrode measurements. The  $\text{Ca}^{2+}$ -selective microelectrode was mounted on a manipulator

(MX-1, Narishige, Tokyo, Japan) connected to a motor-driven hydraulic micromanipulator (MHW-1-4, Narishige, Tokyo, Japan). The movement of the microelectrode was controlled by a MIFE 3 drive box (University of Tasmania, Launceston, Australia). The electrode moved from 30  $\mu\text{m}$  to 130  $\mu\text{m}$  from the leaf surface with frequency of 0.1 Hz. Data were collected at a rate of 20 per second obtained by the MIFE 3 data box (University of Tasmania, Launceston, Australia) working with MIFE software (University of Tasmania, Launceston, Australia). The MIFE software was used for calculations of the net  $\text{Ca}^{2+}$  flux. A basic plane analysis was used. The valid time used in the flux calculation was the last 2 seconds of the applied 10-second intervals. The placement of the microelectrode near the leaf surface was observed under the microscope Nikon Eclipse TE300 (Nikon, Tokyo, Japan). The application of glutamate initially evoked a noise in the recordings lasting approx. 1 minute, which were not included in the figures.

#### Fluorescence measurements

The imaging of the whole *Physcomitrella patens* GCaMP3 mutants was carried out with the use of a Nikon SMZ18 fluorescence stereomicroscope equipped with a Nikon DS-Ri2 16.25 MPix digital color camera and a Nikon SHR Plan Apo 1.6x WD:30 objective (Nikon Instruments Co., Tokyo, Japan). Images and films were collected with NIS-Elements AR (version 5.20.00) software (Nikon Instruments Co., Tokyo, Japan). For fluorescence excitation, a metal arc lamp Prior lumen 200 (Prior Scientific Instruments Ltd, Cambridge, England) with a  $470\pm 20$  nm filter and a 495 dichroic mirror were used. Fluorescence emission images were collected with a  $525\pm 50$  nm barrier filter and exposure time of 200 ms.

The single cell imaging of *Physcomitrella patens* GCaMP3 mutants was carried out on the LSM780 confocal system (Zeiss, Jena, Germany) coupled to an AxioObserver Z.1 inverted microscope equipped with a Plan-Apochromat 63x/1.40 Oil DIC M27 objective. Time-lapse imaging of single cells of *Physcomitrella patens* GCaMP3 mutants was carried out using a 488 nm Argon laser as excitation light and a PMT detector working at a 500–550 nm range. Simultaneous images of cells in the transmission light mode were collected. The pixel dwell time was 1.27 $\mu\text{s}$ . The pinhole diameter was set to 1 AU.

#### Funding

This work was supported by the National Science Centre, Poland, project DAINA 1 No. 2017/27/L/NZ1/03164 entitled "Long-distance electrical signaling systems in plants - adaptation to the change from water to terrestrial environment" and by the European Regional Development Fund under the Operational Program Innovative Economy, project No. POIG.02.02.00-00-025/09 (<http://www.nanofun.edu.pl/en.html>) entitled "National Multidisciplinary Laboratory of Functional Nanomaterials" - 'NanoFun'.

## Disclosures

Conflicts of interest: No conflicts of interest declared

## Acknowledgments

We would like to thank Dr. Thomas J. Kleist for giving us a the transgenic lines of *Physcomitrella patens* expressing GCaMP3. We also thank Mr. Wojciech Staniszewski from PRECOPTIC Co. for sharing the equipment for fluorescence imaging of the whole plant.

## Author contribution

M.K. conceived and designed the work, prepared the main part of experiments, analyzed and interpreted the data, and drafted the main part of the work. P.W. participated in preparation and analysis of the membrane potential measurements. K.D. participated in preparation and analysis of the fluorescence imaging experiments. M.T. revised the work. K.T. participated in writing and revised the work.

## References

- Beilby, M.J., (1985) Potassium channels at *Chara* plazmalemma. *J. Exp. Bot.* 36:228-239.
- Beilby, M.J. (1986) Potassium channels and different states of *Chara* plasmalemma. *J Membr Biol.* 89: 241–249.
- De Bortoli, S., Teardo, E., Szabò, I., Morosinotto, T., and Alboresi, A. (2016) Evolutionary insight into the ionotropic glutamate receptor superfamily of photosynthetic organisms. *Biophys Chem.* 218: 14–26.
- Cove, D. (2000) The moss, *Physcomitrella patens*. *J Plant Growth Regul.* 19: 275–283.

- Dennison, K.L., and Spalding, E.P. (2000) Glutamate-gated calcium fluxes in *Arabidopsis*. *Plant Physiol.* 124: 1511–1514.
- Ermolayeva, E., Hohmeyer, H., Johannes, E., and Sanders, D. (1996) Calcium-dependent membrane depolarisation activated by phytochrome in the moss *Physcomitrella patens*. *Planta.* 199: 352–358.
- Ermolayeva, E., Sanders, D., and Johannes, E. (1997) Ionic mechanism and role of phytochrome-mediated membrane depolarisation in caulonemal side branch initial formation in the moss *Physcomitrella patens*. *Planta.* 201: 109–118.
- Felle, H.H., and Zimmermann, M.R. (2007) Systemic signalling in barley through action potentials. *Planta.* 226: 203–214.
- Haley, A., Russell, A.J., Wood, N., Allan, A.C., Knight, M., Campbell, A.K., et al. (1995) Effects of mechanical signaling on plant cell cytosolic calcium. *Proc Natl Acad Sci.* 92: 4124–4128.
- Johannes, E., Ermolayeva, E., and Sanders, D. (1997) Red light-induced membrane potential transients in the moss *Physcomitrella patens*: Ion channel interaction in phytochrome signalling. *J Exp Bot.* 48: 599–608.
- Kleist, T.J., Cartwright, H.N., Perera, A.M., Christianson, M.L., Lemaux, P.G., and Luan, S. (2017) Genetically encoded calcium indicators for fluorescence imaging in the moss *Physcomitrella* : GCaMP3 provides a bright new look. *Plant Biotechnol J.* 15: 1235–1237.
- Koselski, M., Trebacz, K., Dziubinska, H., and Krol, E. (2008) Light- and dark-induced action potentials in *Physcomitrella patens*. *Plant Signal Behav.* 3: 13–18.
- Koselski, M., Wasko, P., Kupisz, K., and Trebacz, K. (2019) Cold- and menthol-evoked membrane potential changes in the moss *Physcomitrella patens* : influence of ion channel inhibitors and phytohormones. *Physiol Plant.* 167: 433–446.
- Król, E., Dziubińska, H., Trębacz, K., Koselski, M., and Stolarz, M. (2007) The influence of glutamic and aminoacetic acids on the excitability of the liverwort *Conocephalum conicum*. *J Plant Physiol.* 164: 773–784.
- Lacombe, B., Becker, D., Hedrich, R., DeSalle, R., Hollmann, M., Kwak, J.M., et al. (2001) The identity of plant glutamate receptors. *Science* 292: 1486–1487.
- Lam, H.M., Chiu, J., Hsieh, M.H., Meisel, L., Oliveira, I.C., Shin, M., et al. (1998) Glutamate-receptor genes in plants. *Nature.* 396: 125–126.
- Li, F., Wang, J., Ma, C., Zhao, Y., Wang, Y., Hasi, A., et al. (2013) Glutamate receptor-like

- channel3.3 is involved in mediating glutathione-triggered cytosolic calcium transients, transcriptional changes, and innate immunity responses in *Arabidopsis*. *Plant Physiol.* 162: 1497–509.
- Meyerhoff, O., Müller, K., Roelfsema, M.R.G., Latz, A., Lacombe, B., Hedrich, R., et al. (2005) AtGLR3.4, a glutamate receptor channel-like gene is sensitive to touch and cold. *Planta.* 222: 418–427.
- Mousavi, S.A.R., Chauvin, A., Pascaud, F., Kellenberger, S., and Farmer, E.E. (2013) Glutamate receptor-like genes mediate leaf-to-leaf wound signalling. *Nature.* 500: 422-+.
- Ortiz-Ramirez, C., Michard, E., Simon, A.A., Damineli, D.S.C., Hernandez-Coronado, M., Becker, J.D., et al. (2017) Glutamate receptor-like channels are essential for chemotaxis and reproduction in mosses. *Nature.* 549: 91–95.
- Qi, Z., Stephens, N.R., and Spalding, E.P. (2006) Calcium entry mediated by GLR3.3, an *Arabidopsis* glutamate receptor with a broad agonist profile. *Plant Physiol.* 142: 963–971.
- Rensing, S.A., Lang, D., Zimmer, A.D., Terry, A., Salamov, A., Shapiro, H., et al. (2008) The *Physcomitrella* genome reveals evolutionary insights into the conquest of land by plants. *Science* 319: 64–69.
- Reski, R., and Abel, W.O. (1985) Induction of budding on chloronemata and caulonemata of the moss, *Physcomitrella patens*, using isopentenyladenine. *Planta.* 165: 354–358.
- Russell, A.J., Cove, D.J., Trewavas, A.J., and Wang, T.L. (1998) Blue light but not red light induces a calcium transient in the moss *Physcomitrella patens* (Hedw.) B., S. & G. *Planta.* 206: 278–283.
- Russell, A.J., Knight, M.R., Cove, D.J., Knight, C.D., Trewavas, A.J., and Wang, T.L. (1996) The moss, *Physcomitrella patens*, transformed with apoaequorin cDNA responds to cold shock, mechanical perturbation and pH with transient increases in cytoplasmic calcium. *Transgenic Res.* 5: 167–170.
- Saidi, Y., Finka, A., Muriset, M., Bromberg, Z., Weiss, Y.G., Maathuis, F.J.M., et al. (2009) The heat shock response in moss plants is regulated by specific calcium-permeable channels in the plasma membrane. *Plant Cell.* 21: 2829–2843.
- Salvador-Recatalà, V., Tjallingii, W.F., and Farmer, E.E. (2014) Real-time, *in vivo* intracellular recordings of caterpillar-induced depolarization waves in sieve elements using aphid electrodes. *New Phytol.* 203: 674–684.

- Sivaguru, M., Pike, S., Gassmann, W., and Baskin, T.I. (2003) Aluminum rapidly depolymerizes cortical microtubules and depolarizes the plasma membrane: Evidence that these responses are mediated by a glutamate receptor. *Plant Cell Physiol.* 44: 667–675.
- Stolarz, M., Król, E., and Dziubińska, H. (2015) Lithium distinguishes between growth and circumnutation and augments glutamate-induced excitation of *Helianthus annuus* seedlings. *Acta Physiol Plant.* 37: 69.
- Stolarz, M., Krol, E., Dziubinska, H., and Kurenda, A. (2010) Glutamate induces series of action potentials and a decrease in circumnutation rate in *Helianthus annuus*. *Physiol Plant.* 138: 329–338.
- Storti, M., Costa, A., Golin, S., Zottini, M., Morosinotto, T., and Alboresi, A. (2018) Systemic Calcium wave propagation in *Physcomitrella patens*. *Plant Cell Physiol.* 59: 1377–1384.
- Teardo, E., Segalla, A., Formentin, E., Zanetti, M., Marin, O., Giacometti, G.M., et al. (2010) Characterization of a plant glutamate receptor activity. *Cell Physiol Biochem.* 26: 253–262.
- Tester, M. (1988) Pharmacology of K<sup>+</sup> channels in the plasmalemma of the green alga *Chara corallina*. *J Membr Biol.* 103: 159–169.
- Toyota, M., Spencer, D., Sawai-Toyota, S., Jiaqi, W., Zhang, T., Koo, A.J., et al. (2018) Glutamate triggers long-distance, calcium-based plant defense signaling. *Science* 361: 1112–1115.
- Trebacz, K., Simonis, W., and Schonknecht, G. (1994) Cytoplasmic Ca<sup>2+</sup>, K<sup>+</sup>, Cl<sup>-</sup>, and NO<sub>3</sub><sup>-</sup> activities in the liverwort *Conocephalum conicum* L at rest and during action potentials. *Plant Physiol.* 106: 1073–1084.
- Tucker, E.B., Lee, M., Alli, S., Sookhdeo, V., Wada, M., Imaizumi, T., et al. (2005) UV-A induces two calcium waves in *Physcomitrella patens*. *Plant Cell Physiol.* 46: 1226–1236.
- Verret, F., Wheeler, G., Taylor, A.R., Farnham, G., and Brownlee, C. (2010) Calcium channels in photosynthetic eukaryotes: implications for evolution of calcium-based signalling. *New Phytol.* 187: 23–43.
- Wang, G., Hu, C., Zhou, J., Liu, Y., Cai, J., Pan, C., et al. (2019) Systemic root-shoot signaling drives jasmonate-based root defense against nematodes. *Curr Biol.* 29: 3430-3438.e4.

## Figure legends

**Fig. 1.** Representative recordings of glutamate-induced membrane potential changes in *Physcomitrella patens* leaf cells. The measurements were carried out in two-compartment chambers, which facilitated separation of rhizoids and the apical part of the plant. The arrows indicate the moment of application of 5 mM glutamate. The standard solution contained (in mM) 1 KCl, 1 CaCl<sub>2</sub>, 50 sorbitol, and 2 Hepes, pH 7.5 (buffered by Tris). The graph shows the site of insertion of the microelectrode, application of glutamate, and position of the barrier. Apart from one recording (placed in frame), all others present acropetally propagated responses.

Fig. 2. Membrane potential changes in *Physcomitrella patens* leaf cells evoked by glutamate applied at different concentrations: 0.05, 0.5, 5, and 30 mM. The standard solution and captions are the same as in Fig. 1.

Fig. 3. Comparison of the effects of aspartate (5 mM) and glutamate (5 mM) application on membrane potential changes in *Physcomitrella patens* leaf cells. The standard solution and captions are the same as in Fig. 1.

Fig. 4. Representative glutamate-induced membrane potential changes in *Physcomitrella patens* leaf cells recorded at high external chloride and potassium concentrations. The standard solution and captions are the same as in Fig. 1. The inset in the lower panel shows the effect of glutamate stimulation during permanent depolarization of the cell membrane.

**Fig. 5.** Membrane potential changes evoked by glutamate recorded in *Physcomitrella patens* protonema cells. The photographs at the top of the figure present the thread-like chain of

protonema cells studied in the experiment. The micropipette used for microinjection of 5 mM glutamate mixed with 1 mM methyl blue and the microelectrode are indicated (white arrows). Four moments of glutamate injection were chosen - before the stimulation (A), immediately after the application of glutamate (B), after the stimulation of other cells by shifting the micropipette closer the microelectrode (C), and after the application of glutamate directly to the cell where the microelectrode was inserted. All four moments are marked in the membrane potential recordings presented at the bottom of the figure. The inset presents the whole response where the moment of removal of the injecting micropipette from the measuring chamber is indicated by the arrow. The standard solution was the same as in Fig. 1. A movie presenting the whole experiment can be found in Supplementary Video S1.

**Fig. 6.** Fluorescence measurements carried out on protonema cells of *Phycomitrella patens* GCaMP3 mutants. A drop of standard solution supplemented with 5 mM glutamate was placed on an agar plate containing a thread-like chain of protonema cells. The border of the drop is indicated by the dashed white line. Fluorescence was measured in three regions (ROIs). In the upper panel, the red ROI was placed in the site of application of the drop, and blue and green ROIs were placed at a closer and further distance from the border of the drop, respectively. The inset presents the intensity of the fluorescence recorded in three selected ROIs. The color of the curve corresponds to the color of ROI. The dashed line indicates the moment when maximal fluorescence intensity was recorded. The lower panel shows further experiments that were carried out on the same agar plate by application of the drop in a different place. The green ROI from the lower panel was placed in the same region as in the upper panel. A movie presenting the whole experiment can be found in Supplementary Video S3.

**Fig. 7.** Glutamate-induced calcium increase in protonema cells of *Physcomitrella patens* GCaMP3 mutants. Time-lapse images of protonema cells taken before (0 s) and after stimulation (30 s and 63 s). Upper panel fluorescence images, lower panel - merge. The plot indicates the intensity of fluorescence recorded in two regions (ROIs) indicated in the lower panel. The color of the curve corresponds to the color of ROI. The dashed line indicates the time of recorded maximal fluorescence intensity. A movie presenting the whole experiment can be found in Supplementary Video S6.

**Fig. 8.** Net  $\text{Ca}^{2+}$  flux in *Physcomitrella patens* leaf cells treated with 5 mM glutamate. The measurements were carried out in a chamber, which separated rhizoids and the apical part of the plant. The moment of application of glutamate is marked by an arrow. The application of glutamate initially evoked a noise in the recordings lasting approx. 1 minute, which was discarded. The graph shows the location of the  $\text{Ca}^{2+}$ -selective microelectrode, position of the barrier, and the site of glutamate application.

### Supplementary Video Legends

**Supplementary Video 1.** Propagation of the electrical signal between protonema cells. The video demonstrates the effect of microinjection of 5 mM glutamate stained with 1 mM methyl blue onto a chain of protonema cells. The videos from the microscope presenting glutamate application and electrical signal recordings are presented in the left and right panel, respectively. The timescale (in seconds) is located on the upper left side of the video.

**Supplementary Video 2.** Control measurements demonstrating the effect of 1 mM methyl blue on membrane potential changes in protonema cells. The course of the experiment was the same as in Supplementary Video 1.

**Supplementary Video 3.** Glutamate-induced increase in the intracellular  $\text{Ca}^{2+}$  concentration in protonema cells. The video presents the effect of application of a drop of 5 mM glutamate onto the surface of agar with the protonema cells of GCaMP3 mutants. Drops of glutamate were applied in two different places on the agar plate. The timescale (in seconds) is located on the upper left side of the video.

**Supplementary Video 4.** Influence of glutamate on intracellular  $\text{Ca}^{2+}$  concentration changes in leaf cells. The fluorescence measurements were carried out on GCaMP3 mutants. The effects of application and removal of a 5 mM and 30 mM glutamate drop are presented. The timescale (in seconds) is located on the upper left side of the video.

**Supplementary Video 5.** Comparison of the effects of aspartate and glutamate on the increase in the intracellular  $\text{Ca}^{2+}$  concentration. The timescale (in seconds) is located on the upper left side of the video.

**Supplementary Video 7.** Effect of focused glutamate application to protonema cells on an increase in the intracellular  $\text{Ca}^{2+}$  concentration. Glutamate (5 and 30 mM) stained with 1 mM methyl blue was microinjected on a chain of protonema cells. The fluorescence measurements were carried out on GCaMP3 mutants. Fluorescence, transmission light and merge are presented

from the left to the right. The timescale (in seconds) is located on the bottom left side of the video.

**Supplementary Video 8.** Control measurements demonstrating the effect of 1 mM methyl blue on changes in the intracellular  $\text{Ca}^{2+}$  concentration. The course of the experiment was the same as in Supplementary Video 7.

**Supplementary Video 8.** Increase in the intracellular  $\text{Ca}^{2+}$  concentration evoked by mechanical stimulation of gametophyte cells. The stem of the gametophyte of GCaMP3 mutants was bent with a syringe needle. The timescale (in seconds) is located on the upper left side of the video.

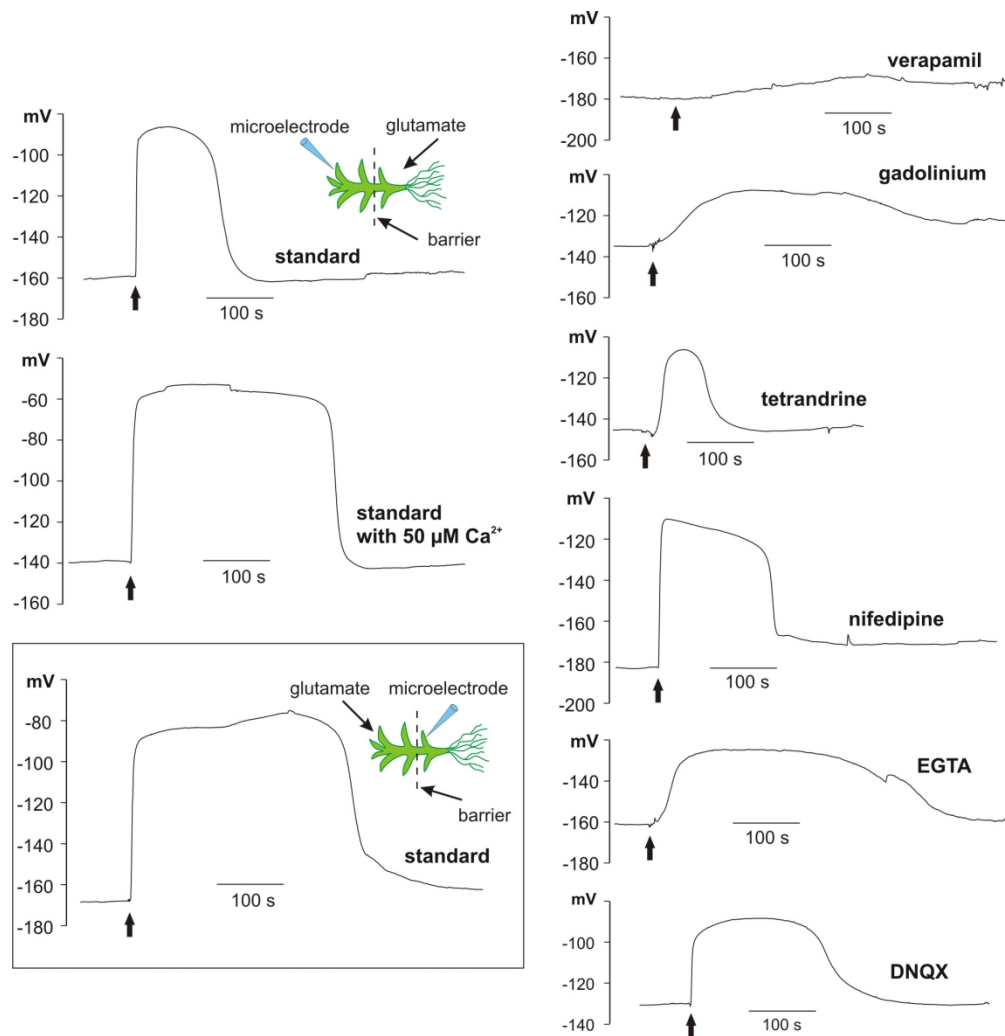


Fig. 1. Representative recordings of glutamate-induced membrane potential changes in *Physcomitrella patens* leaf cells. The measurements were carried out in two-compartment chambers, which facilitated separation of rhizoids and the apical part of the plant. The arrows indicate the moment of application of 5 mM glutamate. The standard solution contained (in mM) 1 KCl, 1 CaCl<sub>2</sub>, 50 sorbitol, an 2 Hepes, pH 7.5 (buffered by Tris). The graph shows the site of insertion of the microelectrode, application of glutamate, and position of the barrier. Apart from one recordings (placed in frame), all others present acropetally propagated responses.

173x178mm (300 x 300 DPI)

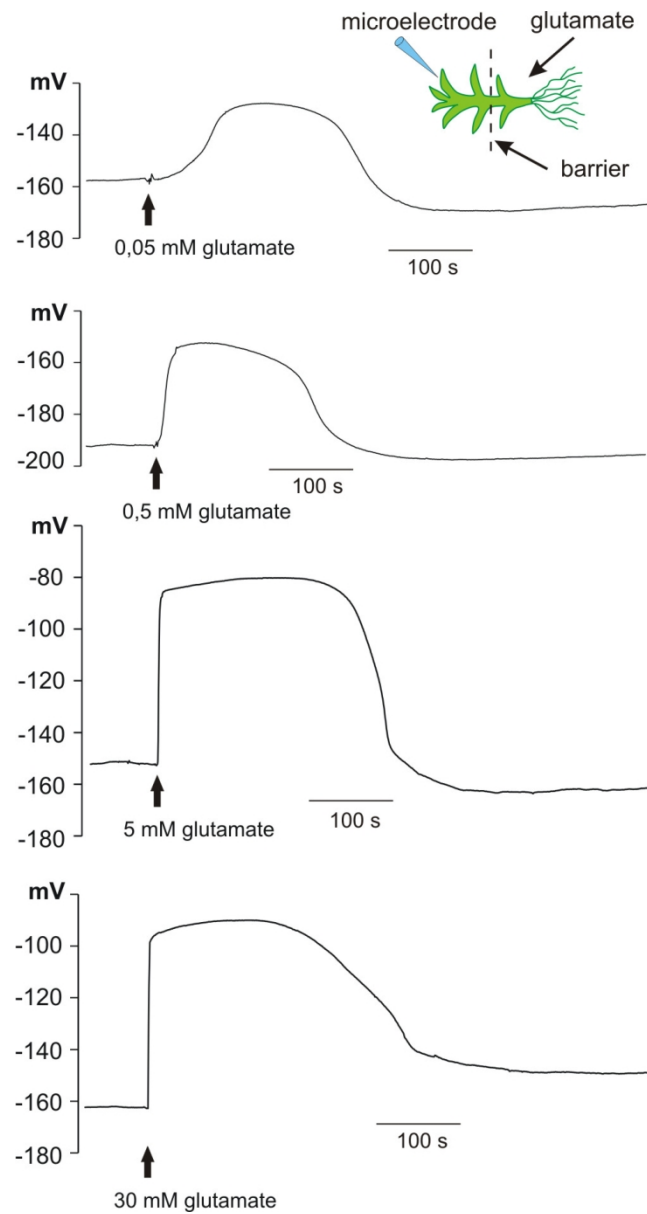


Fig. 2. Membrane potential changes in *Physcomitrella patens* leaf cells evoked by glutamate applied at different concentrations: 0.05, 0.5, 5, and 30 mM. The standard solution and captions are the same as in Fig. 1.

86x160mm (300 x 300 DPI)

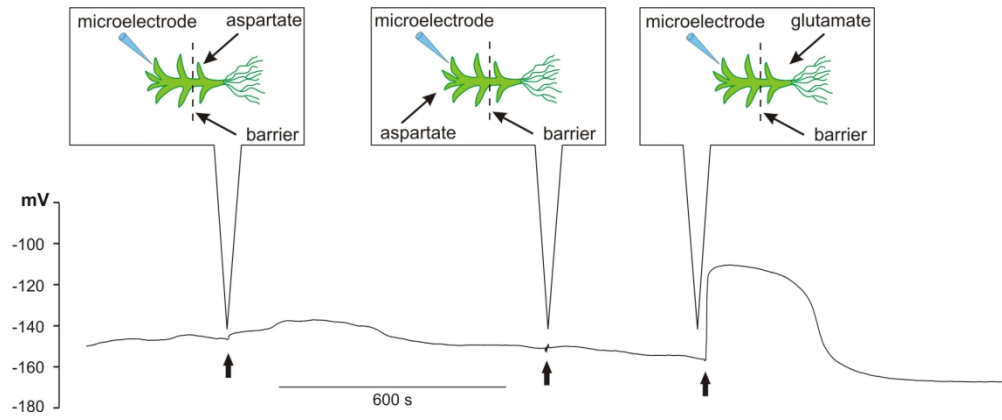


Fig. 3. Comparison of the effects of aspartate (5 mM) and glutamate (5 mM) application on membrane potential changes in *Physcomitrella patens* leaf cells. The standard solution and captions are the same as in Fig. 1.

173x70mm (300 x 300 DPI)

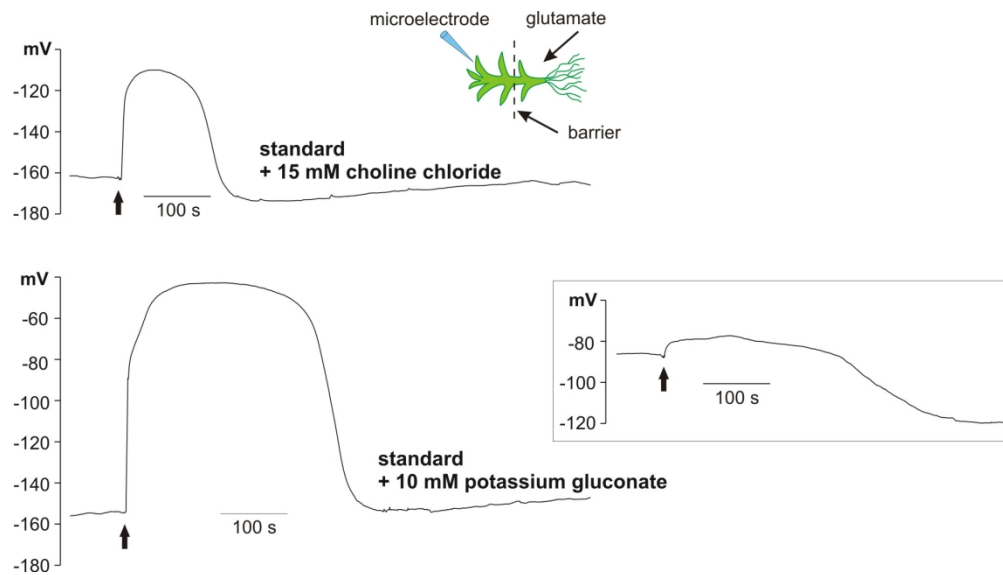


Fig. 4. Representative glutamate-induced membrane potential changes in *Physcomitrella patens* leaf cells recorded at high external chloride and potassium concentrations. The standard solution and captions are the same as in Fig. 1. The inset in the lower panel shows the effect of glutamate stimulation during permanent depolarization of the cell membrane.

173x97mm (300 x 300 DPI)

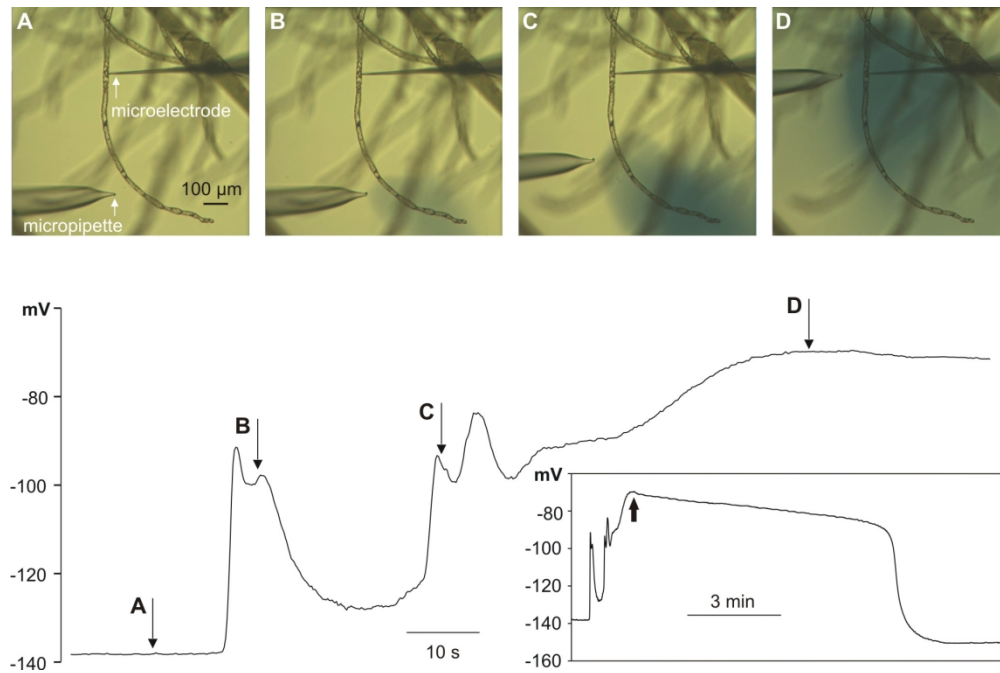


Fig. 5. Membrane potential changes evoked by glutamate recorded in *Physcomitrella patens* protonema cells. The photographs at the top of the figure present the thread-like chain of protonema cells studied in the experiment. The micropipette used for microinjection of 5 mM glutamate mixed with 1 mM methyl blue and the microelectrode are indicated (white arrows). Four moments of glutamate injection were chosen - before the stimulation (A), immediately after the application of glutamate (B), after the stimulation of other cells by shifting the micropipette closer the microelectrode (C), and after the application of glutamate directly to the cell where the microelectrode was inserted. All four moments are marked in the membrane potential recordings presented at the bottom of the figure. The inset presents the whole response where the moment of removal of the injecting micropipette from the measuring chamber is indicated by the arrow. The standard solution was the same as in Fig. 1. A movie presenting the whole experiment can be found in Supplementary Video S1.

173x115mm (300 x 300 DPI)

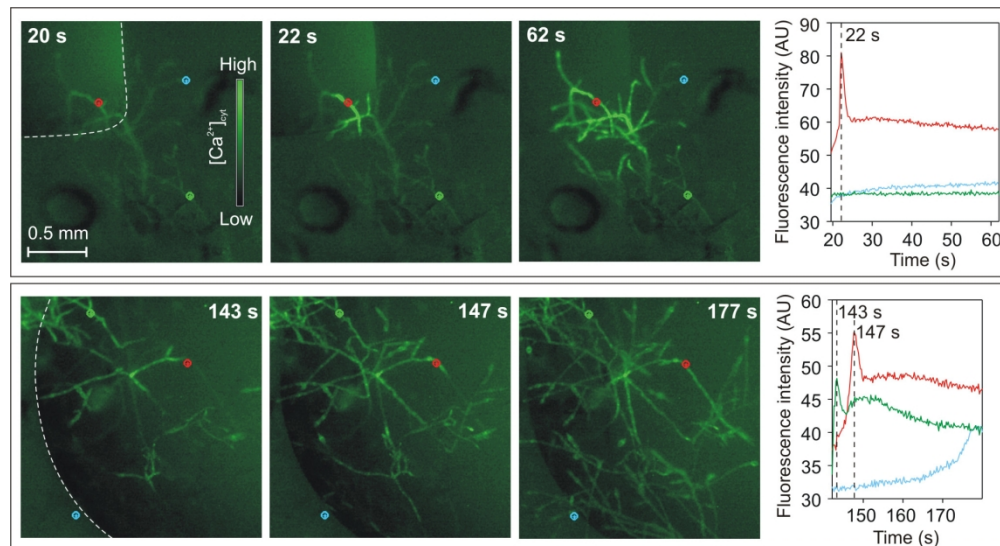


Fig. 6. Fluorescence measurements carried out on protonema cells of *Phycomitrella patens* GCaMP3 mutants. A drop of standard solution supplemented with 5 mM glutamate was placed on an agar plate containing a thread-like chain of protonema cells. The border of the drop is indicated by the dashed white line. Fluorescence was measured in three regions (ROIs). In the upper panel, the red ROI was placed in the site of application of the drop, and blue and green ROIs were placed at a closer and further distance from the border of the drop, respectively. The inset presents the intensity of the fluorescence recorded in three selected ROIs. The color of the curve corresponds to the color of ROI. The dashed line indicates the moment when maximal fluorescence intensity was recorded. The lower panel shows further experiments that were carried out on the same agar plate by application of the drop in a different place. The green ROI from the lower panel was placed in the same region as in the upper panel. A movie presenting the whole experiment can be found in Supplementary Video S3.

173x94mm (300 x 300 DPI)

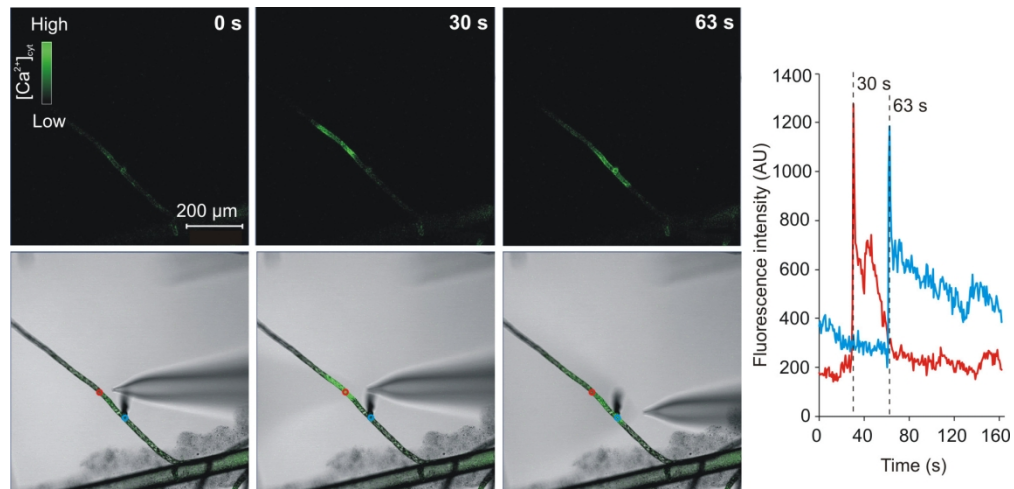


Fig. 7. Glutamate-induced calcium increase in protonema cells of *Physcomitrella patens* GCaMP3 mutants. Time-lapse images of protonema cells taken before (0 s) and after stimulation (30 s and 63 s). Upper panel fluorescence images, lower panel - merge. The plot indicates the intensity of fluorescence recorded in two regions (ROIs) indicated in the lower panel. The color of the curve corresponds to the color of ROI. The dashed line indicates the time of recorded maximal fluorescence intensity. A movie presenting the whole experiment can be found in Supplementary Video S6.

174x83mm (300 x 300 DPI)

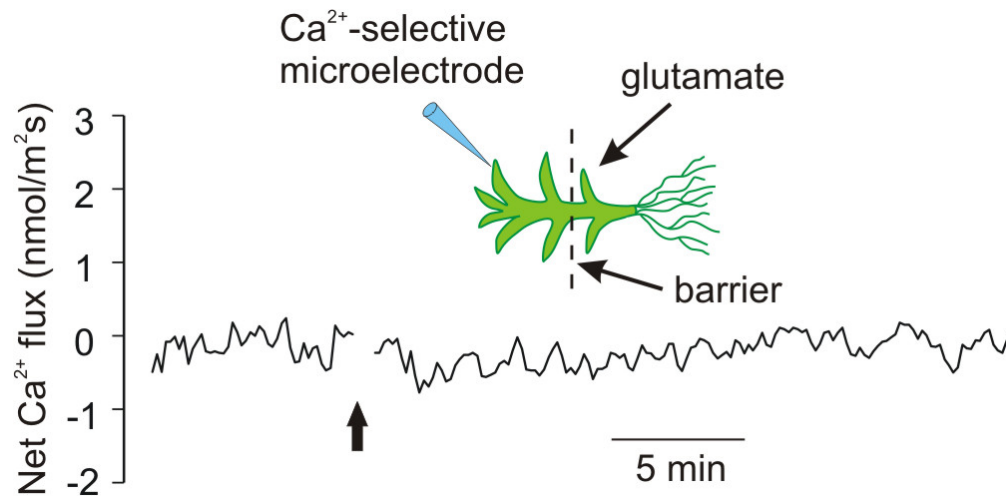


Fig. 8. Net Ca<sup>2+</sup> flux in *Physcomitrella patens* leaf cells treated with 5 mM glutamate. The measurements were carried out in a chamber, which separated rhizoids and the apical part of the plant. The moment of application of glutamate is marked by an arrow. The application of glutamate initially evoked a noise in the recordings lasting approx. 1 minute, which was discarded. The graph shows the location of the Ca<sup>2+</sup>-selective microelectrode, position of the barrier, and the site of glutamate application.

84x41mm (300 x 300 DPI)

**Table 1. Values of parameters describing glutamate-induced long-distance responses recorded in different conditions**

	5 mM glutamate as stimulus	5 mM glutamate as stimulus (basipetal)	0.05 mM glutamate as stimulus	0.5 mM glutamate as stimulus	30 mM glutamate as stimulus	50 $\mu$ M Ca <sup>2+</sup>	10 mM KGluko- nate	15 mM Choline Cl	200 $\mu$ M DNQX	100 $\mu$ M vera- pamil	5 mM GdCl <sub>3</sub>	40 $\mu$ M tetrandrine	100 $\mu$ M nife- dipine	400 $\mu$ M EGTA
<b>V<sub>0</sub></b> (mV)	-163±3 n=26	<b>-174±3*</b> n=9	-174±4 n=6	-169±6 n=8	-165±2 n=14	-160±3 n=12	<b>-150±3*</b> n=10	-158±3 n=11	<b>-140±4*</b> n=16	<b>-180±3*</b> n=14	<b>-144±5*</b> n=10	-158±5 n=12	-167±4 n=14	<b>-134±7*</b> n=9
<b>V<sub>max</sub></b> (mV)	-104±4 n=26	-117±13 n=9	<b>-127±8*</b> n=6	<b>-130±9*</b> n=8	-93±6 n=14	<b>-75±6*</b> n=12	<b>-45±4*</b> n=10	-109±6 n=11	-95±6 n=16	-	-110±6 n=10	-116±7 n=12	-111±8 n=14	-101±4 n=9
<b>A</b> (mV)	59±4 n=26	57±13 n=9	47±8 n=6	<b>38±7*</b> n=8	72±6 n=14	<b>85±5*</b> n=12	<b>105±5*</b> n=10	49±6 n=11	<b>45±4*</b> n=16	-	<b>34±4*</b> n=10	<b>41±6*</b> n=12	55±8 n=14	<b>33±6*</b> n=9
<b>R<sub>dep</sub></b> (mV/s)	13.5±2.3 n=26	<b>3.3±1.4*</b> n=9	<b>0.22±0.04*</b> n=6	<b>1±0.3*</b> n=8	<b>23.1±3.6*</b> n=13	6.7±1.3 n=11	18.9±3.3 n=10	8.9±2.1 n=11	6.8±1.5 n=16	-	<b>0.5±0.1*</b> n=10	<b>1.4±0.3*</b> n=12	10±3 n=14	<b>1.1±0.4*</b> n=9
<b>t<sub>1/2</sub></b> (s)	154±12 n=26	<b>246±57*</b> n=9	173±10 n=6	161±8 n=8	<b>290±33*</b> n=14	<b>334±47*</b> n=11	<b>393±39*</b> n=8	132±16 n=11	206±32 n=16	-	<b>246±53*</b> n=7	<b>97±9*</b> n=11	146±36 n=14	<b>457±82*</b> n=7
<b>Eff (%)</b>	100	82	60	80	100	100	100	100	100	0	71	100	100	56
<b>N</b>	26	11	10	10	14	12	13	11	16	14	14	12	14	16

Table Footnote: The values denote means  $\pm$  standard error. Bold and asterisks indicate statistically significant differences ( $p \leq 0.05$ ). The statistical analysis was prepared using the Mann-Whitney Rank Sum test.  $V_0$  - value of the membrane potential recorded before stimulation,  $V_{max}$  - maximum value of the membrane potential recorded during the response, A - amplitude of response,  $R_{dep}$  - the rate of depolarization,  $t_{1/2}$  - duration of response measured at half of the amplitude, Eff - effectiveness of response evoking, n - number of recorded responses, N - number of tested plants